International Communications in Heat and Mass Transfer 39 (2012) 781–785

Contents lists available at SciVerse ScienceDirect

International Communications in Heat and Mass Transfer

journal homepage: www.elsevier.com/locate/ichmt

Thermal modeling and design for microchannel cold plate with high temperature uniformity subjected to multiple heat sources ☆

Xiaobing Luo *, Zhangming Mao

School of Energy and Power Engineering, Huazhong University of Science & Technology, Wuhan, Hubei, 430074, China

ARTICLE INFO

Available online 25 May 2012

Keywords:
Thermal modeling
Microchannel
Temperature uniformity
Multiple heat sources

ABSTRACT

A compact thermal model was established to model thermal characterization of a microchannel cold plate for high temperature uniformity in multiple heat sources. Analytical calculation of the compact model was presented. Experiments were also conducted to validate the model. The comparison reveals that the measured temperatures are close to the ones predicted by the compact thermal model. The cold plate can help multiple heat sources achieve high temperature uniformity, and the maximum temperature difference among the heat sources is 1.3 °C in the present experimental cases. Moreover, a straight minichannel cold plate was designed and tested under the same flow rate. The measured results show that there exists relatively large temperature gap among the heat sources, and the maximum value is 6.7 °C.

1. Introduction

Size shrinking and multi-functions of electronic devices result in high heat flux. To guarantee their reliability, junction temperature of chips should be maintained at a relatively low level, which requires novel cooling solutions. Microchannel cooling is one of the solutions for its compaction and enhanced cooling performance. Microchannel heat sink was first introduced by Tuckerman and Pease [1]. Since then, many researches have been conducted mainly on heat transfer and pressure drop in microchannels [2]. Reviews [3,4] presented many research works on heat transfer and pressure drop characteristics of regular microchannels.

Unlike regular microchannels, fractal tree-like microchannel is a special kind of microchannel, which was inspired from natural systems, like mammalian circulatory and respiratory systems. Bejan and Errera [5] first studied fractal tree-like microchannels for electronic cooling applications, and they found that a fractal tree-like microchannel has the minimal resistance path for fluid flow. Chen and Cheng [6] analyzed heat transfer and pressure drop in fractal tree-like microchannel nets. It was found that the fractal tree-like channel net has stronger heat transfer capability and requires a lower pumping power, comparing to the traditional parallel channel net. Chen and Cheng [7] also did an experimental investigation on the thermal efficiency of fractal tree-like microchannel nets. The results confirmed that thermal efficiency of fractal tree-like microchannel heat sink is much higher than that of traditional parallel microchannel heat sink when having the same heat transfer rate, temperature difference and inlet velocity. Studies conducted by Pence [8] and Senn et al. [9] obtained the same conclusions as Chen and Cheng [7].

In most actual applications, microchannel substrate or cooling plate with microchannels is used to cool electronic devices with multiple heat sources. For those cases, it is important to reduce temperature gap among heat sources to guarantee performance uniformity of devices. For example, in high power LED and laser applications, the small temperature difference between the LED and laser chips will assure high reliability and good optical performance. So far, little study has been focused on finding the method to achieve temperature uniformity of microchannel substrate for multiple heat sources cooling. Ma et al. [10] did a thermal analysis and modeling of lighting emitting diode (LED) array integrated with as liquid-cooling module. Yuan et al. [11] analyzed thermal performance of high power LEDs array with microchannel cooler. They used more staggered fins in the middle and downstream of the microchannel cooler to increase heat transfer area and achieve uniform temperature for LEDs array.

A compact thermal model, which is used to model a kind of fractal tree-like microchannel cold plate with multiple heat sources, was presented in our previous work [12]. In that work, simulation results were obtained to prove the feasibility of the model. This paper will use this model to design a fractal tree-like minichannel cold plate with high temperature uniformity subjected to multiple heat sources. Meanwhile, a parallel straight minichannel cold plate was also tested at the same working condition to provide a reference for temperature uniformity comparison of the fractal tree-like minichannel cold plate.

2. Compact thermal model

2.1. Thermal resistances network

Structure of the rectangular fractal tree-like microchannel cold plate with multiple heat sources is shown in Fig. 1. The microchannel

☆ Communicated by P. Cheng and W.Q. Tao.

* Corresponding author.
E-mail address: Luoxb@mail.hust.edu.cn (X. Luo).

0735-1933/$ – see front matter © 2012 Elsevier Ltd. All rights reserved.
doi:10.1016/j.icheatmasstransfer.2012.05.007

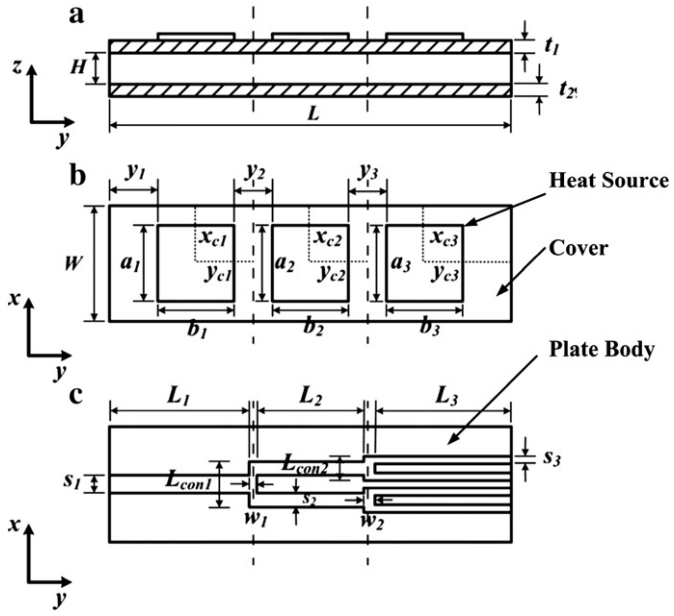

Fig. 1. Geometrical structure of the system (a) staggered section view, (b) top view of heat source and cover, and (c) top view of plate body.

cold plate is formed by a cover and a plate body, where rectangular fractal tree-like microchannels are fabricated on. Three heat sources are located on top surface of the microchannel cold plate.

In the compact thermal model, there would be no heat exchange between contiguous heat sources since we expect that the heat sources temperature will be uniform. Hence, the multiple heat source system could be separated into three parts by *xz* middle planes of contiguous heat sources. The *xz* middle planes are shown as dashed lines in Fig. 1. In each part, heat from the heat source conducts through the cover, and then one part of the heat transfers to the fluid directly, the rest transfers into the plate body and finally dissipates to the fluid. According to the heat transfer processes in the three separated parts, three thermal resistance networks were established as shown in Fig. 2.

To calculate thermal resistance of the plate body conveniently, the plate body is divided into ten blocks by three *xz* middle planes and seven *yz* middle planes along three levels of microchannels. The ten blocks are numbered as 1–6 shown in Fig. 2. Blocks with the same sizes are given the same number. The thermal resistances from R_1 to R_6 are the ones of the numbered "T" shape blocks. Two half "T" shape blocks can be considered as an integrated "T" shape block. As a result, R_1 is thermal resistance of a "T" shape block united by the two blocks with number 1. Likewise, R_2 and R_4 are thermal resistances of "T" shape blocks combined by blocks with numbers 2 and 4, respectively. R_{cov1} to R_{cov3} are thermal resistances of separated cover. R_{h1}–R_{h3} are convective film thermal resistances with fluid. T_{j1}–T_{j3} are junction temperatures or average temperatures of the area where heat sources are located. Q_1–Q_3 are input heating power of the heat sources. T_{f1}–T_{f3} are mean fluid temperatures in three levels of microchannels.

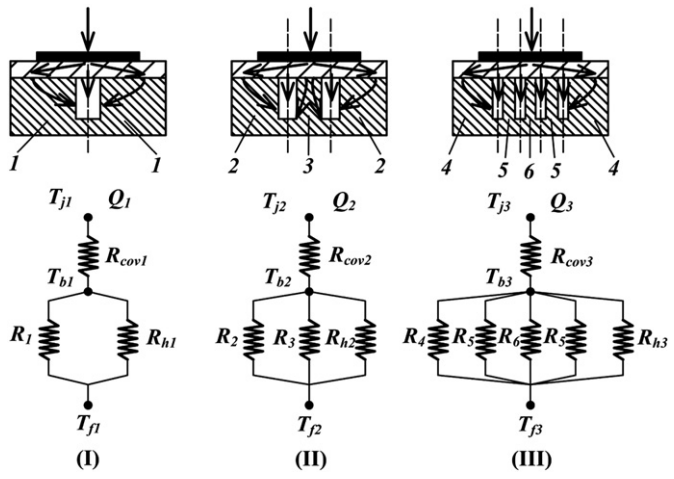

Fig. 2. Thermal resistance networks of the separated parts.

2.2. Calculation of thermal resistances

Fig. 3 shows a "T" shape block. Based on the heat transfer process, the "T" shape block can be simplified as the upper rectangular block by loading an equivalent heat transfer coefficient at its bottom surface. According to the notes of Fig. 3, the equivalent heat transfer coefficient is given as

$$h_{equ\_T} = \frac{1}{R_l a l} \tag{1}$$

where R_l is thermal resistance of the lower rectangular block, and a and l are the width and length of the upper rectangular block. For the lower rectangular block, we suppose that heat from the upper smaller block flows vertically, and then spreads in horizontal direction, and finally dissipates to the fluid [13]. Therefore, R_l can be considered as a combination of three thermal resistances, which stand for thermal resistances of the three heat transfer processes, respectively. The combination is expressed as

$$R_l = R_{l\_1D} + R_{l\_s} + R_{l\_h}. \tag{2}$$

R_{l_1D} is one-dimensional thermal resistance of a small rectangular block with size $a \times l \times t_2$ and it can be calculated as $t_2/(k_{sub} a l)$, where k_{sub} is thermal conductivity of the plate body. R_{l_h} is the convective film thermal resistance of the lower block and it can be calculated as $1/(h(b-a)l)$, where h is the heat transfer coefficient from part of the top surface and b is the width of the lower block. R_{l_s} is the thermal spreading resistance, which can be calculated by [14]

$$R_{l\_s} = \frac{8}{a^2 b l k_{sub}} \sum_{m=1}^{\infty} \frac{\cos^2\left(\frac{1}{2}\lambda_m b\right) \sin^2\left(\frac{1}{2}\lambda_m a\right)}{\lambda_m^3 \varphi(\lambda_m)} + \frac{8}{b l^3 k_{sub}} \sum_{m=1}^{\infty} \frac{\cos^2\left(\frac{1}{2}\delta_n l\right) \sin^2\left(\frac{1}{2}\delta_n l\right)}{\delta_n^3 \varphi(\delta_n)} + \frac{64}{a^2 b l^3 k_{sub}} \sum_{m}^{\infty} \sum_{n=1}^{\infty} \frac{\cos^2\left(\frac{1}{2}\lambda_m b\right) \sin^2\left(\frac{1}{2}\lambda_m a\right) \cos^2\left(\frac{1}{2}\delta_n l\right) \sin^2\left(\frac{1}{2}\delta_n l\right)}{\lambda_m^2 \delta_n^2 \beta_{m,n} \varphi\left(\beta_{m,n}\right)} \tag{3}$$

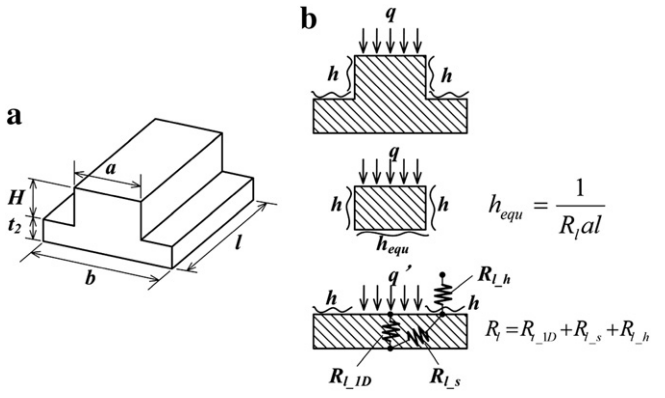

Fig. 3. "T" shape block, (a) geometrical structure, and (b) thermal analysis procedure.

where $\lambda_m = m\pi/b$, $\delta_n = n\pi/l$, $\beta_{m,n} = \sqrt{\lambda_m^2 + \delta_n^2}$, and

$$\varphi(\zeta) = \frac{\zeta \sinh(\zeta t_2) + h/k_{sub}\cosh(\zeta t_2)}{\zeta \cosh(\zeta t_2) + h/k_{sub}\sinh(\zeta t_2)}. \tag{4}$$

ζ is replaced by λ_m, δ_n, and $\beta_{m,n}$ accordingly. Having obtained h_{equ_T} by summing up Eqs. (1)–(4), total thermal resistance of the "T" shape block, which is simplified as the upper block with sides and bottom surface convective cooling, could be calculated by applying expressions presented by Muzychka et al. [15]

$$R_T = \frac{4}{alk_{sub}}\sum_{m=1}^{\infty}\sum_{n=1}^{\infty}\frac{\sin^2\left(\delta_{x,m}\right)\sin\left(\delta_{y,n}\right)\phi}{\delta_{x,m}\delta_{y,n}\gamma_{m,n}\left[\sin\left(2\delta_{x,m}\right)/2+\delta_{x,m}\right]\left[\sin\left(2\delta_{y,n}\right)/2+\delta_{y,n}\right]} \tag{5}$$

where $\delta_{x,m}$, $\delta_{y,n}$, and $\gamma_{m,n} = 2\sqrt{\frac{\delta_{x,m}^2}{a^2}+\frac{\delta_{y,n}^2}{l^2}}$ are the eigenvalues. The eigenvalues are obtained from the following equations

$$\delta_{x,m}\tan\left(\delta_{x,m}\right) = \frac{ha}{2k_{sub}},\ \delta_{y,n}\tan\left(\delta_{y,n}\right) = \frac{hl}{2k_{sub}}. \tag{6}$$

The spreading function ϕ is given as

$$\phi = \frac{\gamma_{m,n}H + \frac{h_{equ\_T}H}{k_{sub}}\tanh\left(\gamma_{m,n}H\right)}{\frac{h_{equ\_T}H}{k_{sub}} + \gamma_{m,n}H\tanh\left(\gamma_{m,n}H\right)} \tag{7}$$

where H is thickness of the upper block. From Eqs. (1)–(7), it is found that R_T is a function of dimensions, thermal properties and boundary conditions of the "T" shape block, and it depends on

$$R_T = f(a, b, l, H, t_2, h, k_{sub}). \tag{8}$$

Hence, thermal resistances of "T" blocks R_1–R_6 can be obtained by inputting parameters accordingly into Eq. (8). h for each "T" shape block will be discussed in Section 2.3.

R_{cov1}–R_{cov3} are thermal resistances of the three separated covers, consisting of one-dimensional thermal resistance and thermal spreading resistance. Here we take R_{cov1} as an example,

$$R_{\mathrm{cov1}} = R_{\mathrm{cov1\_1D}} + R_{\mathrm{cov1\_s}} \tag{9}$$

with

$$R_{con1\_1D} = \frac{t_1}{k_{\mathrm{cov}}(y_1 + b_1 + y_2/2)W} \tag{10}$$

where k_{cov} is the thermal conductivity of the cover, other parameters are shown in Fig. 1. Similarly, we can use the same method to calculate thermal spreading resistance R_{cov1_s}.

2.3. Convective heat transfer in fractal tree-like microchannel

A three-dimensional numerical simulation was performed to analyze heat transfer characteristics in a rectangular fractal tree-like microchannel. The rectangular fractal-tree like microchannel consists of 10 levels of rectangular straight microchannel. The detailed simulation and calculation processes could be referred to reference [12].

To calculate the heat transfer coefficients in the rectangular fractal-tree like microchannel, a new correlation for average Nusselt number was numerically achieved in our previous paper [12]. The new correlation is expressed as

$$Nu_{ave} = \frac{1}{C_1(y^*)^{C_2} + C_3} + C_4, \quad \text{for } 1 \le \alpha \le 10, y^* < y^*_{th} \tag{11}$$

with

$$\begin{cases} C_1 = -8.735\times10^{-4}\alpha^3 + 8.430\times10^{-3}\alpha^2 + 2.709\times10^{-2}\alpha + 2.411 \\ C_2 = -1.153\times10^{-5}\alpha^3 + 1.653\times10^{-4}\alpha - 6.833\times10^{-4}\alpha + 5.760\times10^{-1} \\ C_3 = 1.534\times10^{-4}\alpha^2 - 2.519\times10^{-3}\alpha + 2.369\times10^{-2} \\ C_4 = 6.923 - 1.282\times10^{1}/\alpha + 1.445\times10^{1}/\alpha^2 - 5.585/\alpha^3. \end{cases} \tag{12}$$

Eq. (14) is applied here to predict average Nusselt number of each level of the rectangular fractal-tree like microchannels shown in Fig. 3. Taking level I microchannel for instance, Eq. (11) could be considered as a function of length of microchannel Y, aspect ratio α, and average velocity of fluid u. Thus, Eq. (11) can be expressed as

$$Nu_{ave} = f(Y, \alpha, u). \tag{13}$$

After obtaining the average Nusselt number in each level Nu_i, the heat transfer coefficient in each level microchannel is given by

$$h_i = \frac{k_f Nu_i}{D_{h\_i}} (i = I, II, III) \tag{14}$$

with $D_{h\_i} = 2\ Hs_i/(H + s_i)$, where s_i is the width of the rectangular microchannel in every level.

To model heat transfer in the connective microchannel simply, average Nusselt number in the connective microchannel is presented by the mean value of the local Nusselt number at the end of the pre-level microchannel and the one at the beginning of the next level microchannel. The heat transfer coefficient in the other levels can also be calculated similarly. After obtaining the heat transfer coefficients in the channels, the average ones for calculating thermal resistances in the networks can be achieved.

2.4. Summary of the compact thermal model

After obtaining thermal resistances in network I, II and III, junction temperature, or average temperature of the heat source area, can be calculated as the following equations:

$$\begin{cases} T_{j1} = Q_1\left(R_{\mathrm{cov1}} + \dfrac{1}{\frac{1}{R_1}+\frac{1}{R_{h1}}}\right) + T_{f1} \\ T_{j2} = Q_2\left(R_{\mathrm{cov2}} + \dfrac{1}{\frac{1}{R_2}+\frac{1}{R_3}+\frac{1}{R_{h2}}}\right) + T_{f2} \\ T_{j3} = Q_3\left(R_{\mathrm{cov3}} + \dfrac{1}{\frac{1}{R_4}+\frac{2}{R_5}+\frac{1}{R_6}+\frac{1}{R_{h3}}}\right) + T_{f3} \end{cases} \tag{15}$$

where Q_1–Q_3 are input heating powers of the three heat sources, respectively; T_{f1}–T_{f3} are average fluid temperature in the three levels of microchannel, respectively. T_{f1}–T_{f3} can be calculated with the principle of energy conservation between the heat source and the fluid.

3. Experimental setup and error analysis

The aim of establishing the compact thermal model is applying the model to design the fractal tree-like microchannel and obtain high temperature uniformity among heat sources. To validate the present model, a fractal tree-like minichannel cold plate was designed according to the optimized results by the model. To provide a comparison, a straight rectangular minichannel cold plate was also designed and fabricated for experiments. The geometrical structure and dimensions of the two cold plates are shown in Fig. 4(a) and

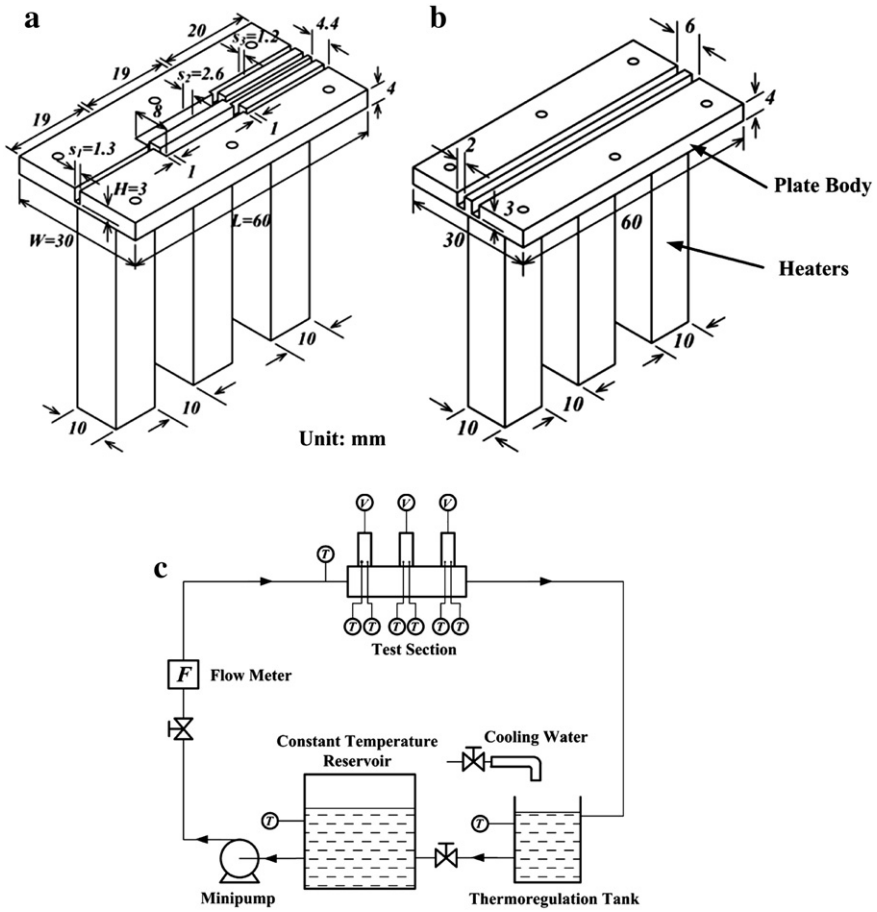

Fig. 4. Schematic of (a) tree-like channel plate body, (b) straight rectangular minichannel plate body and (c) experimental apparatus.

Fig. 4(b), in which the cover boards are not shown. Both the cover board and the plate body were made of copper.

Fig. 4(c) is the schematic diagram of the experimental apparatus, which includes test section, flow meter, minipump, constant temperature reservoir, and thermoregulation tank. As shown in Fig. 4(c), water with constant temperature is driven by a minipump and flows through a flow meter and minichannel plate in the test section. After flowing out of the test section, the water is heated and enters into a thermoregulation tank where it can be cooled down to a constant temperature, the same as that in the constant temperature reservoir.

The inlet and outlet pipes are connected to the inlet and outlet of the channel plate. The cold plate includes three blocks where three heaters are put inside to act as heat sources. It is noted here that the three blocks and the channel plate are fabricated and integrated as one body. The channel plate with the pipes is located in a plastic base, which is made up by a base cover and a base body. The channel plate is tightly clinched inside the base body by the base cover.

K type thermocouples were used to measure temperatures. All the thermocouples were connected with a data acquisition system. Before the experiment, the thermal couples were calibrated in an ice bath, and uncertainty of the thermocouples is evaluated as ± 0.3 °C.

The uncertainty of the electrical resistances of the three heaters is $\pm 1\Omega$, and their input voltage uncertainty is ± 0.8 V. Eq. (20) is the calculation expression of the heating power. Eq. (21) is the error propagation formulation based on Eq. (20). According to Eq. (21), uncertainties of the heating power of the three heaters are ± 0.58 W, ± 0.57 W, and ± 0.56 W when they are 30 W. Mass flow of the loop was controlled by valve and the flow meter. Uncertainty of the flow meter is ± 0.1 l/h (liter per hour).

$$Q = V^2/r \tag{20}$$

$$\pm\Delta Q = \pm\left(\frac{2V}{r}\Delta V + \frac{V^2}{r^2}\Delta r\right) \tag{21}$$

4. Comparison results and discussions

The fractal tree-like minichannel cold plate and the straight rectangular minichannel plate were both tested under three groups of working conditions. In the three groups of working conditions, input heating powers of all the three heat sources were the same and varied from 10 W to 30 W, and the incremental step was 2 W. Flow rate was the only variable parameter among the three groups of working conditions, 5.0 l/h in the first group, 6.5 l/h in the second group, and 7.2 l/h in the last group. Both flows in the fractal tree-like minichannel and the straight minichannel were laminar because of the small channel size.

Fig. 5(a) shows the temperatures of the three heat sources when the fractal tree-like millichannel plate worked under one constant flow rate. The similar data at other flow rates is also obtained, but not shown in this paper. From Fig.5(a), we can see that the heat source temperatures are very close to each other. Other data which is not shown in this paper also proves this. This shows that the uniform temperature distribution is achieved.

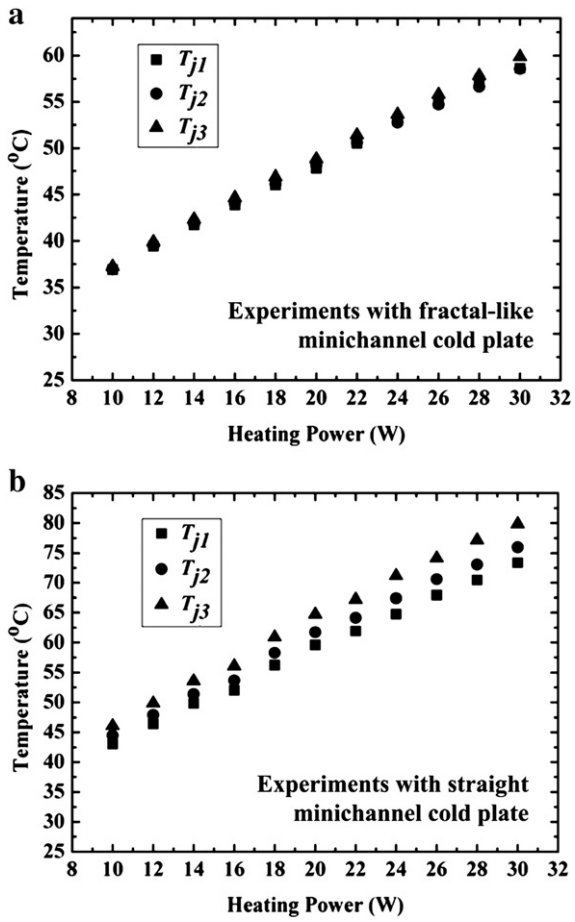

Fig. 5. Temperature variations of three heat sources with the heating power at 5.0 l/h flow rate on (a) fractal tree-like minichannel and (b) straight minichannel.

The compact thermal model was applied to predict the temperatures of the heat sources. Here, one group of modeling results is listed in Table 1, together with the experimental results. As shown in Table 1, good temperature uniformity is achieved among the heat sources for all working conditions. The maximum temperature gap among the three heat sources is 1.3 °C at $Q = 30$ W. The junction temperatures predicted by the compact thermal model are close to the ones obtained by the experiment. With consideration of the experimental errors, we can conclude that the compact thermal model is feasible to achieve temperature uniformity among multiple heat sources for the engineering design of the fractal tree-like microchannel or minichannel.

Table 1
Temperature comparison between experiment and compact thermal model at 5.0 l/h flow rate.

Q (W)	Experiment				Compact thermal model			
	T_{in}(°C)	T_{j1}(°C)	T_{j2}(°C)	T_{j3}(°C)	T_{in}(°C)	T_{j1}(°C)	T_{j2}(°C)	T_{j3}(°C)
10	25.0	36.9	37.0	37.3	25.0	36.7	36.7	37.3
12	25.1	39.4	39.5	39.9	25.0	39.0	39.0	39.7
14	25.3	41.7	41.8	42.3	25.0	41.3	41.4	42.2
16	25.2	43.9	44.0	44.7	25.0	43.7	43.7	44.6
18	25.4	46.0	46.1	46.9	25.0	46.0	46.1	47.1
20	25.1	47.8	48.1	48.8	25.0	48.3	48.4	49.5
22	25.2	50.5	50.6	51.4	25.0	50.6	50.7	51.9
24	25.1	52.9	52.8	53.6	25.0	53.0	53.0	54.3
26	25.1	54.8	54.7	55.8	25.0	55.3	55.3	56.7
28	25.1	56.8	56.6	57.8	25.0	57.6	57.6	59.2
30	25.2	58.6	58.6	59.9	25.0	59.9	60.0	61.6

Fig. 5(b) shows the temperatures of the heat sources when the straight minichannel cold plate worked at 5.0 l/h flow rate. From Fig. 5(b), it can be found that high temperature gaps exist among the heat sources. The temperature gap increases with the heating power increasing.

From the comparison shown in Fig. 5, it is found that the fractal tree-like minichannel cold plate is more helpful than the straight minichannel cold plate to achieve temperature uniformity among heat sources.

5. Summary

A compact thermal model was established to model thermal characteristics of a rectangular fractal tree-like microchannel cold plate for multiple heat sources cooling. A fractal tree-like minichannel cold plate was designed, fabricated and tested based on the compact thermal model. A straight minichannel plate was tested and compared with the fractal tree-like minichannel cold plate under the same working conditions. The comparison reveals that the compact thermal model is valid and useful for the design of fractal tree-like microchannel or minichannel cold plate to achieve temperature uniformity among multiple heat sources. Fractal tree-like microchannel or minichannel cold plate is a better choice to obtain temperature uniformity among multiple heat sources.

Acknowledgment

The authors would like to acknowledge the financial support in part from 973 Project of The Ministry of Science and Technology of China (2009CB320203, 2011CB013105), and in part by the Foundation of State Key Laboratory of Coal Combustion (FSKLCC1103).

References

[1] D.B. Tuckerman, F.W. Pease, High-performance heat sinking for VLSI, IEEE Electronic Device Letters EDL-2 (1981) 126–129.
[2] P.S. Lee, S.V. Garimella, Thermally developing flow and heat transfer in rectangular microchannels of different aspect ratios, International Journal of Heat and Mass Transfer 49 (2006) 3060–3067.
[3] C.B. Sobhan, S.V. Garimella, A comparative analysis of studies on heat transfer and fluid flow in microchannels, Microscale Thermophysical Engineering 5 (2001) 293–311.
[4] S.V. Garimella, C.B. Sobhan, Transport in microchannels — a critical review, Annual Reviews of Heat Transfer 13 (2003) 1–50.
[5] A. Bejan, M.R. Errera, Deterministic tree networks for fluid flow: geometry for minimal flow resistance between a volume and one point, Fractals 5 (1997) 685–695.
[6] Y.P. Chen, P. Cheng, Heat transfer and pressure drop in fractal tree-like microchannel nets, International Journal of Heat and Mass Transfer 45 (2002) 2643–2648.
[7] Y.P. Chen, P. Cheng, An experimental investigation on the thermal efficiency of fractal tree-like microchannel nets, International Communications in Heat and Mass Transfer 32 (2005) 931–938.
[8] D.V. Pence, Reduced pumping power and wall temperature in microchannel heat sinks with fractal-like branching channel networks, Microscale Thermophysical Engineering 6 (4) (2002) 319–330.
[9] S.M. Senn, D. Poulikakos, Laminar mixing, heat transfer and pressure drop in tree-like microchannel nets and their application for thermal management in polymer electrolyte fuel cell, Journal of Power Sources 130 (2004) 178–191.
[10] Z.T. Ma, X.J. Wang, D.Q. Zhu, S. Liu, Thermal analysis and modeling of LED array integrated with an innovative liquid-cooling, *Proc. IEEE 6th ICEPT*, Shenzhen, China, 2005, pp. 1–4.
[11] L.L. Yuan, S. Liu, M.X. Chen, X.B. Luo, Thermal analysis of high power LED array packaging with microchannel cooler, Proc. IEEE 7th ICEPT, Shanghai, China, 2006, pp. 1–5.
[12] Z.M. Mao, X.B. Luo, S. Liu, Compact thermal model for microchannel substrate with high temperature uniformity subjected to multiple heat sources, Proc. IEEE 61th ECTC, Lake Buena Vista, FL,USA, 2011, pp. 1662–1672.
[13] X.B. Luo, Z.M. Mao, S. Liu, Analytical thermal resistances model for eccentric heat source on rectangular plate with convective cooling at upper and lower surfaces, International Journal of Thermal Sciences 50 (2011) 2198–2204.
[14] Y.S. Muzychka, J.R. Culham, M.M. Yovanovich, Thermal spreading resistance of eccentric heat sources on rectangular flux channels, IEEE Journal of Electronic Packaging 125 (2003) 178–185.
[15] Y.S. Muzychka, J.R. Culham, M.M. Yovanovich, Thermal spreading resistances in rectangular flux channels part II-edge cooling, Proc. 36th AIAA Thermophysics Conference, Orlando, Florida, USA, AIAA-2003-4188, 2003, pp. 1–9.